Quantum confinement effects in Ge [110] nanowires

S. P. Beckman,* Jiaxin Han, and James R. Chelikowsky
Center for Computational Materials, Institute for Computational Engineering and Sciences, Departments of Physics and Chemical Engineering, University of Texas, Austin, Texas 78712, USA
(Received 23 May 2006; published 11 October 2006)

The effect of dimensional confinement on quantum levels is investigated for hydrogenated Ge [110] nanowires by "density-functional-theory pseudopotential" methods. The energy band dispersion is presented for wires up to 2.8 nm in diameter. By placing a H_2 molecule in vacuum for reference the bands of the different sized wires are aligned and compared. It is found that for wires with diameters smaller than 3 nm, confinement strongly affects the shape and energies of the conduction bands. It is found that the energy of the valence-band maximum does not change with diameter once a wire is greater than 2.0 nm. The valence band maximum scales with diameter D as $\propto D^{-2.2}$, and the conduction band scales as $\propto D^{-0.8}$.

DOI: 10.1103/PhysRevB.74.165314 PACS number(s): 71.20.Mq, 73.21.Hb, 78.20.Bh

Quantum confinement in one or more dimensions results in unique electronic and phonotic properties, which may lead to the development of next-generation devices. Within the past five years significant progress has been made in the development of low-dimensional devices including the development of ballistic carbon nanotube transistors[1] and high-performance Ge- and Si-nanowire field-effect transistors.[2,3] There is potential for nanowires to be used as highly sensitive biological and chemical sensors.[4] Logic gates have been assembled from nanowire building blocks.[5] High-efficiency solar cells have been created from self-assembled Ge dot structures.[6] In this work we focus on nanowire science.

It is known that quantum confinement strongly affects the optical properties of nanowires. Experimentally much work has been performed studying the optical properties of these wires. Although measurements of the photoluminescence spectra of free-standing Si nanowires have been produced,[7] little progress has been made in the study of the optical properties of Ge nanowires. It is believed that states at the Ge-Ge oxide interface as well as states from metal contaminants provide numerous sites for nonradiative recombination events. Recent attempts to measure the photoluminescence spectra from free-standing Ge wires grown on Si substrates have resulted in spectra originating from the Ge-Si interface, not the Ge wires themselves.[8] Other studies of the optical properties of Ge nanowires have focused on non-free-standing structures. The photoluminescence spectra have been observed for one-dimensional (1D) structures grown along the edge of steps on a Si substrate.[9] Other studies have measured the photoluminescence spectra of Ge wires confined to the pores of hexagonal mesoporous silica.[10]

The investigation of the optical properties of Ge nanowires can be aided by computational methods. Numerous computational studies have been performed to investigate the optical properties of nanocrystals.[11–14] Similar studies have focused on the absorption spectra of Si nanowires.[15] Preliminary investigations of Ge nanowires have begun and are available in the literature.[16,17] These studies have employed all-electron potentials[16] and the GW corrections[17] and hence have been focused exclusively on small-diameter wires.

Here we investigate the effects of confinement on [110] Ge nanowires, using "density-functional-theory pseudopotential" methods. We examine wires with diameters as large as 2.8 nm and observe how the $E(\mathbf{k}_z)$ dispersions evolve as the diameter changes. We align the bands in wires of different diameters and show how dimensional confinement affects the valence and conduction bands, respectively.

The density-functional-theory pseudopotential methods used here are encoded in ABINIT.[18,19] The exchange and correlation functional is treated within the local density approximation.[20,21] The wave function is expressed as a plane-wave summation truncated at an energy cutoff of 19 a.u. (atomic units with $e=\hbar=m=1$ and energy units of hartree).

For Ge, a Troullier-Martins pseudopotential form is used with $4s^24p^24d^0$ valence and radial cutoff of $r_s/r_p/r_d = 2.6/2.5/2.8$ a.u.[22] Partial core corrections are included with a core cutoff of 1.98 a.u.[23] The pseudopotential is transformed into local and nonlocal components by the Kleinman-Bylander transformation with the p channel selected as the local component.[24] This pseudopotential predicts a cubic lattice parameter a_{cubic} of 10.62 a.u., which is within 0.7% of the experimental value of 10.70 a.u.[25] The elasticity parameters are calculated to be (in GPa) $c_{11}=129.4$, $c_{12}=49.98$, and $c_{44}=67.62$, which is accurate to within 5% of the experimental values $c_{11}=129.2\pm1.2$, $c_{12}=47.9\pm1.2$, and $c_{44}=67.0\pm0.7$.[26]

Using this pseudopotential, the electronic structure of bulk Ge is calculated and presented in Fig. 1. Although it is known that the local density approximation underestimates band gaps, at least to a qualitative level the structure is correct. In particular the relative ordering of the L, Γ, and X conduction-band minima (CBM) is correct.[27] The difference between the highest occupied molecular orbital and lowest unoccupied molecular orbital (the HOMO-LUMO gap) for bulk Ge is predicted to be 0.44 eV. This corresponds to the transition from the Γ-point valence-band maximum (VBM) to the CBM at L. The Kohn-Sham eigenvalues $E(\mathbf{k})$ are calculated across the entire Brillouin zone and projected in the $\mathbf{k}=[110]$ direction to produce the projected band structure, shown in Fig. 2. In the limit that a [110] wire's diameter approaches infinity the electronic structure will approach this bulk projected structure. It is apparent in Fig. 2 that when projected in the [110] direction the Ge band gap is direct, unlike in the bulk crystal. This is because the CBM at L ($[\bar{1}11]$,$[1\bar{1}1]$,$[\bar{1}1\bar{1}]$,$[1\bar{1}\bar{1}]$) maps onto Γ. The CBM is de-

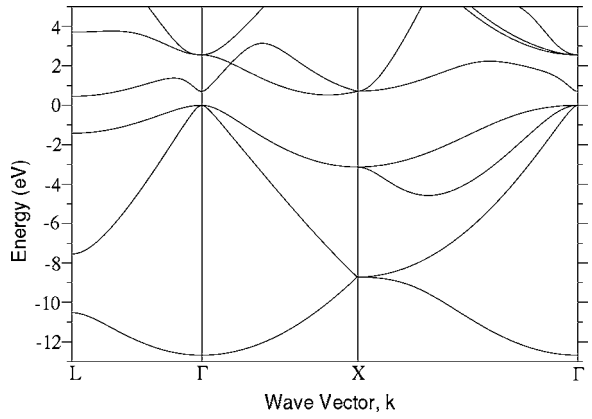

FIG. 1. The band structure of Ge calculated within pseudopotential density-functional theory. The energy zero is taken arbitrarily to be the VBM.

generate because the L minima at ($[111]$ $[\bar{1}\bar{1}1]$,$[11\bar{1}]$,$[\bar{1}\bar{1}\bar{1}]$) project onto the Brillouin zone edge. For wires smaller than 3 nm, confinement effects increase the energy of the conduction bands at the Brillouin-zone edge, leaving only one CBM, at Γ. For wires with diameters larger than 3 nm, the double minima is an important feature in the band structure.

The geometries of the Ge wires investigated are shown in Fig. 3. The diameter is taken to be the average dimension of the parallelogram's diagonals, which are (in nm) 0.47, 1.37, and 2.8 for the three wires studied. This cross-sectional shape is chosen to maximize the area of low-energy {111} surfaces; however, it is believed that wires with diameter larger than 1.5 nm prefer a hexagonal shape.[28,29] The wire shape chosen for this study may not be optimal, but it is known that the band structures for these parallelogram-shaped wires are similar to those calculated for hexagonal wires.[30] There is an uncertainty in identifying the cross-sectional diameter of the structures. For the wires in Figs. 3(d), 3(b), and 3(a) the cross-sectional diameters range (in nm) from 0.34 to 0.42, 1.1 to 1.6, and 2.1 to 3.2, respectively. We propose that the diagonal measure of the wire is a good approximation because it is the largest dimension that will produce the narrowest features of the band edges. Confinement in the $[111]$ and $[\bar{1}\bar{1}2]$ directions will produce features inside the bands. A region of at least 12.2 a.u. of vacuum buffers the wires in neighboring cells in the x and y directions. The translational periodicity along the wires, in the z direction, is $\frac{\sqrt{2}}{2}a_{cubic}$. Sampling three unique points in the k_z direction is sufficient for total energy convergence to better than 1 meV.

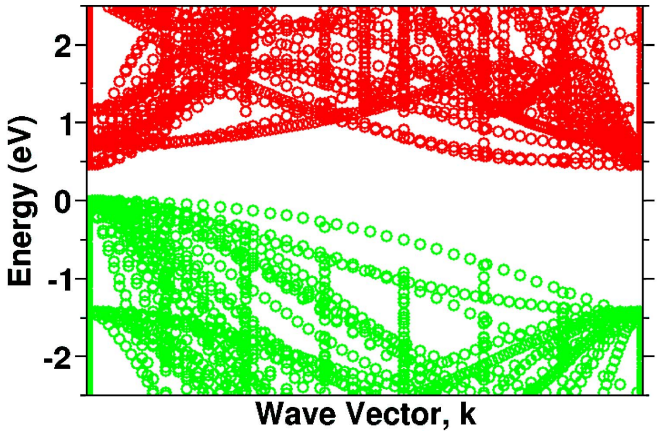

FIG. 2. (Color online) The band structure of Ge projected in the [110] direction.

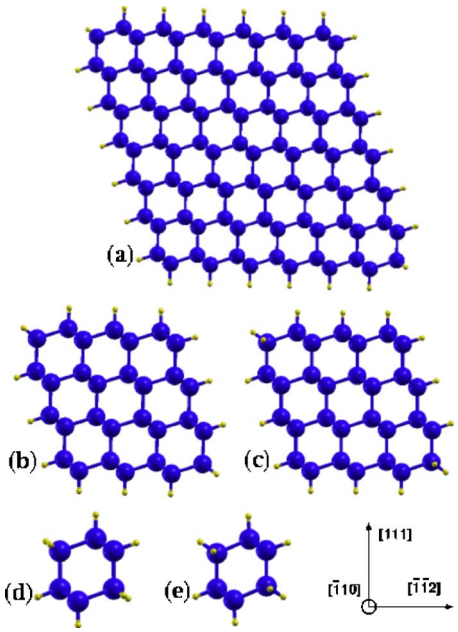

FIG. 3. (Color online) The cross sections of the [110] Ge wires studied: (a) 2.8 nm diameter, (b) 1.37 nm diameter, (c) 1.37 nm diameter with full internal relaxation, (d) 0.47 nm diameter, and (e) 0.47 nm diameter with full internal relaxation.

The positions of the atoms are selected according to the lattice parameter calculated for bulk Ge. The surfaces are passivated with hydrogen positioned to eliminate surface states from the gap. Hence, the calculations predict the effect of confinement on the HOMO-LUMO gap, while suppressing surface effects. To examine the influence of internal structural relaxation, the two smallest wires are fully relaxed, shown in Figs. 3(c) and 3(e). Only atoms within one atomic layer of the surface are observed to move, and the most pronounced changes are at the corners of the parallelograms. Comparison of the relaxed and unrelaxed electronic structures reveals a change in the HOMO-LUMO gap of 290 meV for the smallest wire and a 50-meV change for the 1.37-nm wire. The $E(\mathbf{k}_z)$ dispersions for the 0.47 nm wires are plotted in Fig. 4. Qualitatively the shapes of the band edges do not change, yet individual bands are observed to shift. We find the internal relaxation for wires larger than 1.3 nm to be negligible.

In addition to identifying the HOMO-LUMO gap in these wires, it is also desirable to align the bands in the different wires. We increase the vacuum region by 12.5 a.u. in the x direction, and a hydrogen molecule is placed between the wires, as shown in Fig. 5. The molecule is aligned in the y direction with a bond length of 1.5 a.u. The energy dispersion in the k_z direction for an isolated H_2 molecule in a periodic cell with dimensions $15.0\times17.0\times7.5066$ a.u. is

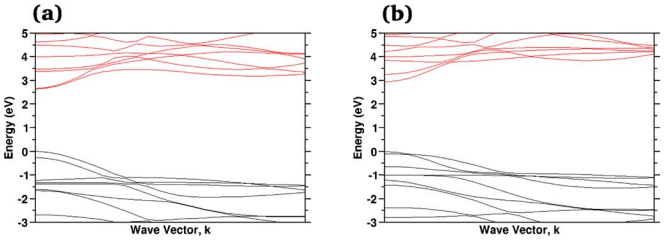

FIG. 4. (Color online) The $E(\mathbf{k})$ dispersion for the 0.47-nm-diam wires. The energy zero is set arbitrarily to be at the VBM. (a) is the band structure calculated by holding the Ge fixed according to the bulk crystal structure. (b) shows the bands calculated when the entire wire structure is allowed to relax to minimize the total energy.

shown in Fig. 6. We find that the states are flat and nearly molecular; the H_2 molecular levels are a good reference for aligning the bands. Because all of the wires have the same period in the z direction, any interaction between the hydrogen molecules need not be considered.

The dispersion in the k_z direction for the three wires is plotted in Fig. 7. As the diameter increases, the gap decreases and approachs the predicted bulk band gap. The band edges becomes significantly more bulklike as the diameter increases. At a diameter of 2.8 nm, the conduction bands at the Brillouin-zone edge are almost level with the bands at Γ as predicted for the bulklike bands in Fig. 1. The 1.37-nm and 2.8-nm wires have the same VBM. For Ge nanowires with diameters greater than 1.4 nm, the change in the HOMO-LUMO gap is due entirely to the confinement of the CB states. This is consistent with the CB states being inherently less localized than those of the VB.

Within a simple "particle-in-a-box" model, it is predicted that as the diameter D is changed, the band gap will vary as $\frac{1}{D^2}$. The calculated HOMO-LUMO gap versus the diameter is fit to the function

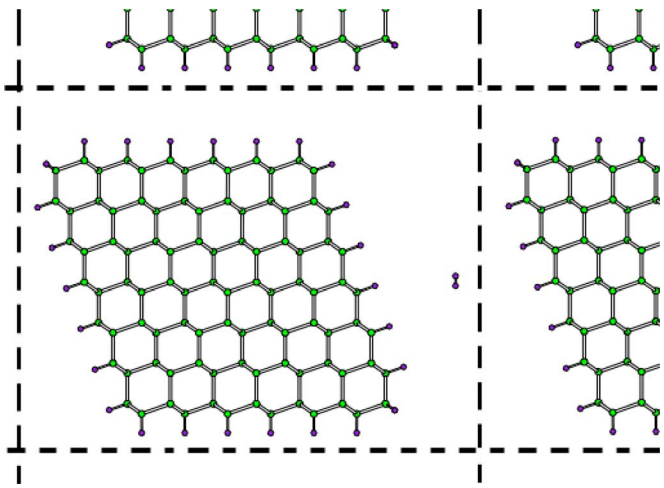

FIG. 5. (Color online) The geometry of the supercell with a H_2 molecule to be used as reference. The dashed lines are the boundaries between the neighboring cells. The distance between the surfaces of wires in neighboring cells and the H_2 molecule is 12.5 a.u.

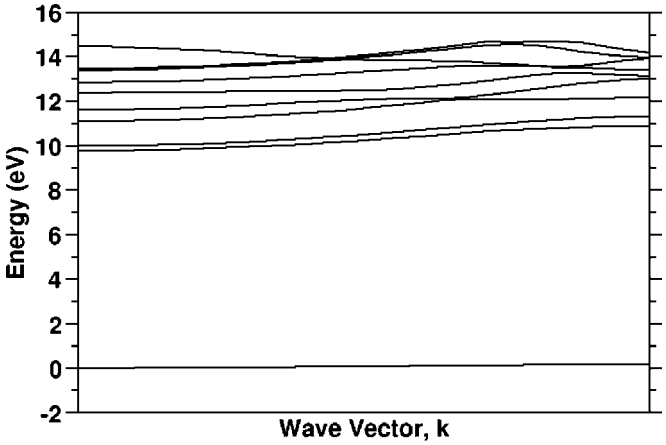

FIG. 6. The local-density-approximation band structure in the k_z direction of an isolated H_2 molecule. The z dimension of the computational cell is selected to have the same periodicity as the Ge [110] wires.

$$E_{gap}(D) = \frac{\alpha}{D^{\beta}} + 0.44, \tag{1}$$

with $\alpha = 1.20$ and $\beta = 0.98$ as is shown in Fig. 8.

In bulk insulating crystals the self-energy correction to the Kohn-Sham eigenstates, solved for within the GW approximation, results in a rigid shift of the bands, effectively opening the band gap to near the experimentally predicted gap.[31] For the work here, such a rigid shift would leave the coefficients α and β unaffected. The effect of confinement on the corrections due to many-body interactions cannot be known *a priori*. It is observed in Si nanowires that confinement results in a larger self-energy correction in smaller-diameter wires.[15] One might postulate that if the GW correction were applied to the results in this paper, a small increase in the value of α, and possibly β, would be observed.

Comparison to previous work indicates the same relative trends.[16,17] We observed that the calculated HOMO-LUMO gap for bulk Ge is highly sensitive to the choice of pseudopotential. This might explain the difference between the cal-

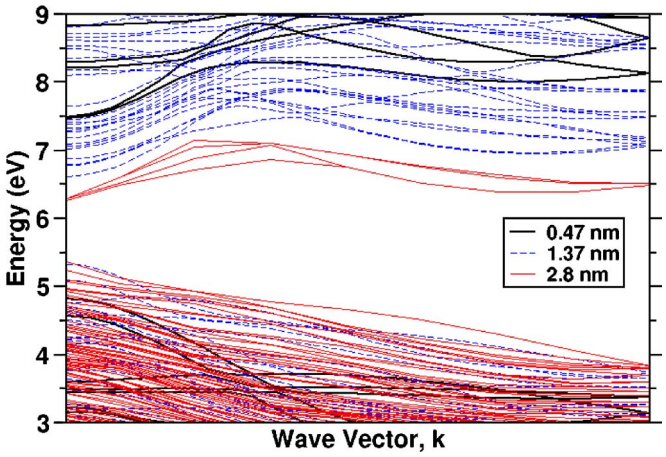

FIG. 7. (Color online) The Kohn-Sham $E(\mathbf{k})$ dispersions for the three wires.

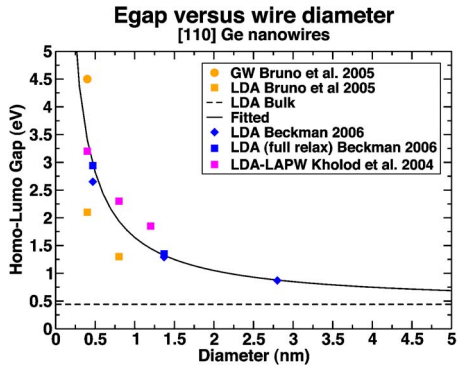

FIG. 8. (Color online) A plot of the calculated HOMO-LUMO gap versus the wire diameter. The solid line is fit to the data calculated in this paper. The Bruno data come from Ref. 17, and the Kholod data come from Ref. 16.

culations of Bruno *et al.*[17] and the present work. The agreement between the all-electron calculation of Kholod *et al.*[16] and the present work, for the smallest-diameter wire, gives us confidence that the pseudopotential approach is as expected. The slight divergence between the previous study[16] and the present work, at larger diameters, can possibly be explained by the difference in wire cross section or by the difference between the pseudopotential and all-electron potentials.

The dependence of the VBM and CBM on D is fit to

$$E_{VBM}(D) = \frac{-0.11}{D^{2.2}} \tag{2}$$

and

$$E_{CBM}(D) = \frac{0.95}{D^{0.8}} + 0.44, \tag{3}$$

with the resulting curves plotted in Fig. 9. It is significant that for small wires, the effect of confinement is greater on the VBM than on the CBM. For large wires, the VBM is relatively unaffected by the wire's diameter and all of the change in the band gap is due to changes in the CBM. Figure 9 shows the response of the VBM and CBM to changes in the wire diameter; however, it is not an indication of the overall effect of confinement on the wave functions. As observed in Fig. 7 changing the wire diameter from 0.47 nm to 1.37 nm significantly affects the shape of the valence band $E(\mathbf{k})$ dispersion, reducing the energy of the states near the Brillouin zone edge by approximately 0.3 eV relative to the VBM. Although the CBM is more sensitive to the diameter than the VBM, the valence states are still strongly affected by quantum confinement.

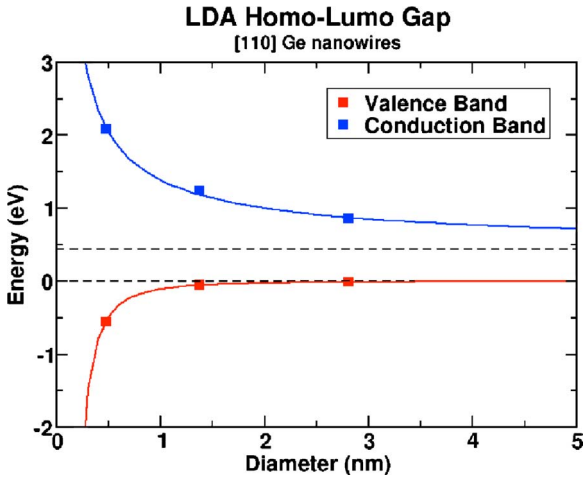

FIG. 9. (Color online) The energy of the VBM and CBM versus wire diameter.

In summary, the energy dispersion for hydrogen-passivated [110] Ge nanowires of different diameters is calculated. Atomic relaxations only occur near the surface of the wire and do not significantly affect the energy bands of wires with diameter greater than 1.3 nm. The HOMO-LUMO gap versus the wire diameter is fit to an appropriate function to allow for the extrapolation of these results to larger-diameter wires. The shape of the band edges becomes bulklike for wires with diameters greater than 2 nm. The CBM becomes twofold degenerate, as predicted from the bulk projected bands, for wires with diameter greater than around 3 nm. The effect of confinement on the CBM and VBM is distinguished by using the molecular levels of H_2 as a reference. Confinement only significantly affects the VBM for wires with diameters less than around 2 nm.

This work was supported in part by the National Science Foundation under Grant No. DMR-0551195 and the U.S. Department of Energy under Grant Nos. DE-FG02-89ER45391 and DE-FG02-03ER15491. Computational resources were provided in part by the National Energy Research Scientific Computing Center (NERSC) and the Texas Advanced Computing Center (TACC).

*Electronic address: sbeckman@ices.utexas.edu; URL: http://www.sbeckman.net/scott

[1] A. Javey, J. Guo, Q. Wang, M. Lundstrom, and H. Dai, Nature (London) **424**, 654 (2003).
[2] D. W. Wang, Q. Wang, A. Javey, R. Tu, H. J. Dai, H. Kim, P. C. McIntyre, T. Krishnamohan, and K. C. Saraswat, Appl. Phys. Lett. **83**, 2432 (2003).
[3] Y. Cui, Z. Zhong, D. Wang, W. U. Wang, and C. M. Lieber, Nano Lett. **3**, 149 (2003).
[4] Y. Cui, Q. Wei, H. Park, and C. M. Lieber, Science **293**, 1289 (2001).
[5] Y. Huang, X. Duan, Y. Cui, L. J. Lauhon, K. Kim, and C. M. Lieber, Science **294**, 1313 (2001).
[6] A. Alguno, N. Usami, T. Ujihara, K. Fujiwara, G. Sazaki, and K. Nakajima, Appl. Phys. Lett. **83**, 1258 (2003).
[7] J. D. Holmes, K. P. Johnston, R. C. Doty, and B. A. Korgel, Science **287**, 1471 (2000).
[8] B. V. Kamenev, V. Sharma, L. Tsybeskov, and T. I. Kamins, Phys.

Status Solidi A **202**, 2753 (2005).
[9] G. Jin, Y. S. Tang, J. L. Liu, and K. L. Wang, J. Vac. Sci. Technol. A **17**, 1406 (1999).
[10] G. Audoit, Éimhín Ní Mhuircheartaigh, S. M. Lipson, M. A. Morris, W. J. Blau, and J. D. Holmes, J. Mater. Chem. **15**, 4809 (2005).
[11] I. Vasiliev, S. Ogut, and J. R. Chelikowsky, Phys. Rev. B **65**, 115416 (2002).
[12] I. Vasiliev, S. Ogut, and J. R. Chelikowsky, Phys. Rev. Lett. **86**, 1813 (2001).
[13] I. Vasiliev, S. Ogut, and J. R. Chelikowsky, Phys. Rev. B **60**, R8477 (1999).
[14] S. Ogut, J. R. Chelikowsky, and S. G. Louie, Phys. Rev. Lett. **79**, 1770 (1997).
[15] X. Zhao, C. M. Wei, L. Yang, and M. Y. Chou, Phys. Rev. Lett. **92**, 236805 (2004).
[16] A. N. Kholod, V. L. Shaposhnikov, N. Sobolev, V. E. Borisenko, F. A. D. Fa, and S. Ossicini, Phys. Rev. B **70**, 035317 (2004).
[17] M. Bruno, M. Palummo, R. Del Sole, V. Olevano, A. N. Kholod, and S. Ossicini, Phys. Rev. B **72**, 153310 (2005).
[18] W. Kohn and L. J. Sham, Phys. Rev. **140**, B1133 (1965).
[19] X. Gonze *et al.*, Comput. Mater. Sci. **25**, 478 (2002).
[20] D. M. Ceperley and B. J. Alder, Phys. Rev. Lett. **45**, 566 (1980).
[21] J. P. Perdew and A. Zunger, Phys. Rev. B **23**, 5048 (1992).
[22] N. Troullier and J. L. Martins, Phys. Rev. B **43**, 1993 (1991).
[23] S. G. Louie, S. Froyen, and M. L. Cohen, Phys. Rev. B **26**, 1738 (1982).
[24] L. Kleinman and D. M. Bylander, Phys. Rev. Lett. **48**, 1425 (1982).
[25] *Semiconductors: Group IV Elements and III-V Compounds*, edited by O. Madelung, Data in Science and Technology (Springer-Verlag, New York, 1991).
[26] W. L. Bond, W. P. Mason, H. J. McSkimin, K. M. Olsen, and G. K. Teal, Phys. Rev. **78**, 176 (1950).
[27] M. L. Cohen and J. R. Chelikowsky, *Electronic Structure and Optical Properties of Semiconductors*, Vol. 75 of Springer Series in Solid-State Sciences (Springer-Verlag, New York, 1988).
[28] T. L. Chan, C. V. Ciobanu, F. C. Chuang, N. Lu, C. Z. Wang, and K. M. Ho, Nano Lett. **6**, 277 (2006).
[29] Y. Wu, Y. Cui, L. Huynh, C. J. Barrelet, D. C. Bell, and C. M. Lieber, Nano Lett. **4**, 433 (2004).
[30] A. J. R. da Silva (private communication).
[31] M. S. Hybertsen and S. G. Louie, Phys. Rev. B **34**, 5390 (1986).